Inorganic Chemistry

ARTICLE

pubs.acs.org/IC

Complex Nanoscale Cage Clusters Built from Uranyl Polyhedra and Phosphate Tetrahedra

Daniel K. Unruh, Jie Ling, Jie Qiu, Laura Pressprich, Melissa Baranay, Matthew Ward, and Peter C. Burns*

Department of Civil Engineering and Geological Sciences, University of Notre Dame, 156 Fitzpatrick Hall, Notre Dame, Indiana 46556, United States

Supporting Information

ABSTRACT: Five cage clusters that self-assemble in alkaline aqueous solution have been isolated and characterized. Each is built from uranyl hexagonal bipyramids with two or three equatorial edges occupied by peroxide, and three also contain phosphate tetrahedra. These clusters contain 30 uranyl polyhedra; 30 uranyl polyhedra and six pyrophosphate groups; 30 uranyl polyhedra, 12 pyrophosphate groups, and one phosphate tetrahedron; 42 uranyl polyhedra; and 40 uranyl polyhedra and three pyrophosphate groups. These clusters present complex topologies as well as a range of compositions, sizes, and charges. Two adopt fullerene topologies, and the others contain combinations of topological squares, pentagons, and hexagons. An analysis of possible topologies further indicates that higher-symmetry topologies are favored.

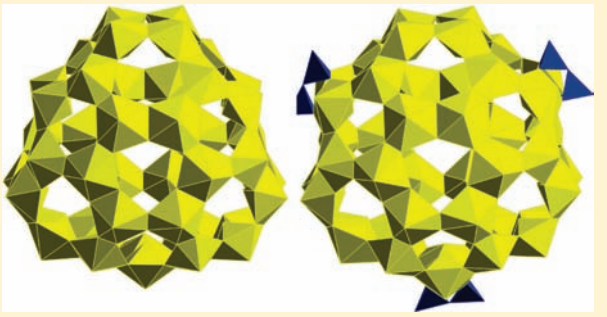

INTRODUCTION

Whereas considerable progress has been made in the development of nanoscale molecular clusters consisting of transition metals[1−4] and C,[5,6] investigations of such materials are in their infancy in actinide chemistry. Given the complex role of f electrons in bonding in actinides and their diverse redox chemistry, the actinide elements will provide fertile landscapes for creation and manipulation of nanoscale molecular clusters. Controlling the behavior of actinide elements on the nanoscale is inherently important as we seek to understand the complex relationships between the structures and properties of nanoscale materials. Such materials hold promise for applications in an advanced nuclear energy cycle.[7]

A variety of studies have incorporated actinide cations into polyoxometalates as linkers between transition metal oxide clusters,[8−15] but few have focused on building clusters specifically from actinide polyhedra. We are executing a systematic combinatorial synthesis program focused on creating complex nanoscale clusters based upon the uranyl ion.[16−21] Our focus is on uranyl ions that are bridged by bidentate peroxide, because a partially covalent interaction between the U^{6+} cations and the peroxide group causes the $U-O_2-U$ dihedral angle to be inherently bent.[18,22] A bent configuration favors self-assembly of nanoscale cage clusters in aqueous solution, rather than the extended sheet structures that are typical of uranyl compounds. We have reported creation and characterization of 16 clusters that are built from uranyl polyhedra, 13 of which are cage clusters.[16−19,23,24] These clusters contain from 16 to 60 uranyl ions and exhibit a broad range of complex topologies that include several fullerenes. We have introduced pyrophosphate and oxalate as linkers in cage clusters built from uranyl ions and reported eight and two clusters with pyrophosphate and oxalate, respectively.[20,21] Some of these are topological derivatives of clusters that contain only uranyl polyhedra, whereas others adopt novel topologies.

Considering the 26 clusters built from uranyl ions that we have reported, as well as our computational studies of fragments of these clusters,[22] it is apparent that the uranyl−peroxide−uranyl bridge is essential for their formation. The local $U-O_2-U$ dihedral angle is to some extent tunable through the size and electronegativity of counterions that coordinate the uranyl ion O atoms, which encourages the assembly of cage clusters with different sizes.[22] Of the myriad of possible graphical isomers for a given number of polyhedra, these cage clusters appear to exhibit a preference for high-symmetry topologies, presumably as this equates to a more even distribution of any structural strain.[23]

We continue to create and characterize cage clusters built from uranyl ions at a previously unexpected high rate. These clusters are furthering our understanding of the roles of counterions, solution conditions, topology, and symmetry in the formation of complex nanoscale clusters. Here, we report five clusters, two of which are built solely from uranyl polyhedra and three of which also contain phosphate tetrahedra. All present new topologies and fresh insights into the complex chemistry of nanoscale clusters of actinides in aqueous solutions.

EXPERIMENTAL PROCEDURES

. ***Caution!*** *Although depleted U was used in the synthesis methods given below, it is mildly radioactive, and appropriate precautions for working with radioactive materials should be followed.*

Received: January 11, 2011
Published: May 19, 2011

Table 1. Selected Crystallographic Data for Clusters

	U_{30a}	$U_{30}Py_6$	$U_{30}Py_{12}P_1$	U_{42}	$U_{42}Py_3$
	$[(UO_2)_{30}(O_2)_{30}(OH)_{30}]^{30-}$	$[(UO_2)_{30}(O_2)_{39}(P_2O_7)_6]^{42-}$	$[(UO_2)_{30}(O_2)_{30}(P_2O_7)_{12}(PO_4)(H_2O)_5]^{51-}$	$[(UO_2)_{42}(O_2)_{42}(OH)_{42}]^{42-}$	$[(UO_2)_{42}(O_2)_{42}(OH)_{36}(P_2O_7)_3]^{48-}$
a (Å)	55.286(5)	19.522(2)	18.793(3)	26.3747(16)	26.605(11)
b (Å)		34.155(5)	27.188(5)	35.341(2)	
c (Å)	20.523(2)	38.237(4)	31.553(6)	39.674(3)	33.08(3)
α (deg)			95.800(2)		
β (deg)			99.525(2)	102.859(1)	
γ (deg)			106.396(2)		
V (Å^3)	54325(9)	25496(5)	15066(5)	36053(4)	20278(20)
space group	$R3m$	$Cmcm$	$P\bar{1}$	$C2/c$	$P6_3/m$
Z	3	4	2	4	1
T (K)	125	125	125	125	125
θ-max (deg)	25.1	16.19	21.5	25.1	26.4
reflns collected	180085	46449	106051	177709	197224
indep. reflns	22208	3467	34300	32056	14074
unique $F_o > 4\sigma$	18603	2752	24624	19917	9671
R_1 (%)	3.65	8.53	14.58	6.31	8.67
wR_2 (%)	9.19	23.18	38.51	18.37	31.44
S	1.01	1.85	2.29	1.02	2.09

Cluster and Crystal Synthesis. Crystals containing each cluster were grown in aqueous solutions created using distilled and Millipore-filtered water with a resistance of 18.2 MΩ cm. The production of crystals was part of a systematic combinatorial synthesis program that included thousands of experiments. Given the large number of synthesis experiments undertaken simultaneously, continuous monitoring was impractical. Crystals may have formed months prior to harvesting in some cases.

Crystals were harvested from their mother liquors that still contained significant concentrations of uranyl ions, as indicated by their yellow color. These crystals facilitated the structural characterization of the clusters by X-ray diffraction.

Crystals containing U_{30a} were obtained from a solution created by adding 4.0 mL of a 0.2 M aqueous uranyl nitrate hexahydrate solution to a 10 mL glass vial, together with 1.5 mL of 30% H_2O_2 followed by vigorous stirring. Subsequently, 3 M aqueous LiOH solution was added dropwise with continuous stirring until a pH of 9.95 was reached. A total of 250 μL of the resulting solution was transferred to a 4 mL glass vial, and 12 μL of 8.5 M RbOH aqueous solution and 1.9 mg of $Ba(OH)_2$ were added. The vial was left open to the air for 24 h, after which it was capped and left standing at room temperature. Square blocky crystals measuring ~200 μm across were collected after 2 years. The solution pH measured at the time of crystal harvesting was 9.9.

Crystals containing U_{42} were obtained from a solution that was created by adding 5.0 mL of 0.2 M aqueous uranyl nitrate hexahydrate solution to a 10 mL glass vial with 1 mL of 0.1 M aqueous $K(IO_3)$, 0.5 mL of 0.2 M aqueous KNO_3, and 0.51 mL of 30% H_2O_2. The pH of the resulting solution was adjusted to 9.82 by adding 1.385 mL of 2.0 M aqueous LiOH together with vigorous stirring, which resulted in a clear solution. A total of 0.333 mL of this solution was transferred to a 4 mL glass vial and was covered with 0.7 mL of chloroform-d in an attempt to promote crystal growth. The vial was left standing and capped at room temperature. Yellow, trapezoidal shaped plates measuring ~200 μm in diameter were present after 1 year. The solution pH measured when the crystals were harvested was 7.7.

Crystals containing cluster $U_{30}Py_6$ were grown from a solution created by mixing 0.1 mL of a 0.5 M aqueous uranyl nitrate solution with 0.1 mL of 30% H_2O_2, 0.1 mL of 2.4 M LiOH, 0.2 mL of 0.5 M aqueous 2,3-dihydroxy-butanedioic acid, and 0.05 mL of 0.5 M aqueous $K_4P_2O_7$, all in a 4 mL glass vial. The solution was initially vigorously stirred until a clear solution resulted that had a pH of 7.2 and was then left open to the atmosphere under ambient conditions. Crystals formed in three weeks with a final solution pH of 7.8, and the vial was capped to prevent evaporation to total dryness.

Crystals containing cluster $U_{30}Py_{12}P_1$ were crystallized from a solution that was created by combining 0.1 mL of 0.5 M aqueous uranyl nitrate, 0.1 mL of 30% H_2O_2, 0.1 mL of 2.4 M LiOH, 0.15 mL of 0.5 M aqueous 2,3-dihydroxy-butanedioic acid, and 0.05 mL of 0.5 M aqueous $K_4P_2O_7$. The resulting mixture was stirred until a clear solution with a pH of 7.8 resulted. It was then allowed to evaporate under ambient conditions, and crystals formed in five weeks, at which time the vial was sealed to prevent further evaporation. The pH of the solution over the crystals was 8.4.

Crystals containing the $U_{42}Py_3$ cluster were grown in a solution that contained 0.3 mL of 0.5 M aqueous uranyl nitrate, 0.3 mL of 30% H_2O_2, 0.2 mL of 2.4 mL LiOH, and 0.1 mL of 0.3 M aqueous KCl. These components were stirred together until a clear solution resulted that had a pH of 8.9. A total of 0.2 mL of this solution, together with 0.075 mL of ultrapure water, 0.03 mL of a 0.1 M aqueous oxalic acid solution, and 0.1 mL of 0.25 M aqueous $K_4P_2O_7$ were combined in a 4 mL glass vial, resulting in a solution with a pH of 8.7. The solution was then allowed to evaporate under ambient conditions, and crystals formed within 5 days, at which time the vial was capped to prevent further evaporation. The pH of the solution over the crystals was 9.2.

Chemical Analysis. Energy dispersive spectra were collected for single crystals containing each cluster using a LEO EVO-50XVP variable-pressure/high-humidity scanning electron microscope. Spectra for each compound confirmed the presence of U, O, P (in the case of three clusters), and counterions except Li (which cannot be detected using this method).

Infrared Spectra. Infrared spectra were obtained for single crystals using a SensIR technology IlluminatIR FT-IR Micro spectrometer. A single crystal of each was placed on a glass slide, and the spectrum was collected following crushing of the crystal with a diamond ATR

objective. The spectra were taken from 650 to 4000 cm^{-1} with a beam aperture of 100 μm. Spectra are given in Figure 10.

X-Ray Diffraction. Crystals containing clusters of uranyl polyhedra contain substantial interstitial water, some of which is lost upon prolonged exposure to the air, which reduces crystal quality. Crystals were isolated from their mother solutions, placed on cryoloops in oil, and mounted on a Bruker PLATFORM three-circle diffractometer equipped with an APEX II CCD detector and graphite monochromatized Mo Kα radiation with a crystal-to-detector distance of 6.0 cm. Crystals were maintained in a stream of nitrogen at ~125 K during data collection. A sphere of data was collected for each crystal using frame widths of 0.5° in ω. Intensity data were corrected for Lorentz, polarization, and background effects using the Bruker program APEX II. Corrections for absorption were applied using the program SADABS. The SHELXTL suite of programs was used for the solution and refinement of the crystal structures.[25]

Structural analysis for cage clusters built from uranyl polyhedra is challenging because of inherent properties of the material. The X-ray scattering is dominated by the U atoms, making precise determination of O atom positions difficult and the location of H atoms impossible. The counterions, as well as H_2O groups located between the clusters of uranyl polyhedra, are usually disordered. The crystals contain significant volumes that have low electron density, which reduces X-ray diffraction intensity. Diffraction data are seldom observed at higher angles (typically above ~45° 2θ for Mo Kα radiation). These various factors combine to give regions of diffraction space with weak or nonobserved reflections. The result is relatively imprecise structure parameters, with bond length errors of 0.02 Å or more. The diffraction data often do not support refinement of anisotropic displacement parameters for the lighter atoms, including O. Despite these various shortcomings, X-ray diffraction studies are the crucial means for determining the polyhedral connectivities and structure topologies of cage clusters built from uranyl polyhedra.[20,21]

The $U_{30}Py_{12}P_1$ clusters crystallize in space group $P\bar{1}$. A direct methods solution provided the positions of the U atoms. The K, P, and O atoms were located in difference Fourier maps calculated following subsequent refinement of partial-structure models. Multiple cycles of refinement and Fourier-map analysis provided an asymmetric unit with 30 U, 266 O, 17 K, and 25 P atoms. Consideration of the bond valences[26] incident upon the O atoms, together with the details of their coordination environments, was used for the identification of O atoms of peroxide groups, O atoms of hydroxyl groups, O atoms of pyrophosphate groups, O atoms of uranyl ions, and O atoms of H_2O groups.

The structures of crystals containing U_{30a}, $U_{30}Py_6$, U_{42}, and $U_{42}Py_3$ clusters were derived from direct methods and subsequent cycles of difference-Fourier maps and least-squares refinement of the models. Refinement of these structures was relatively straightforward. The O atoms were assigned as for the structure of $U_{30}Py_{12}P_1$. Selected crystallographic and refinement parameters are provided in Table 1, with full details of each structure given in the Supporting Information.

Calculation of Possible Isomers. The program CaGe[27] (http://caagt.ugent.be/CaGe) was used to calculate the possible isomers for a given number of vertices within specific boundary constraints. All calculations were constrained to include only closed three-connected vertices.

RESULTS

Cluster Topology and Composition. The 26 different clusters, of which 23 are cage clusters, we have previously reported self-assemble in aqueous solutions over a range of pH conditions. Here, we provide the structures and compositions of five additional cage clusters, two of which contain only uranyl hexagonal bipyramids, and three that are built from uranyl hexagonal bipyramids and phosphate tetrahedra. The cage clusters are designated as U_xV_y, where x designates the number of uranyl ions, V represents one or more chemical species, and y gives the number of each of the V species in the cage cluster.

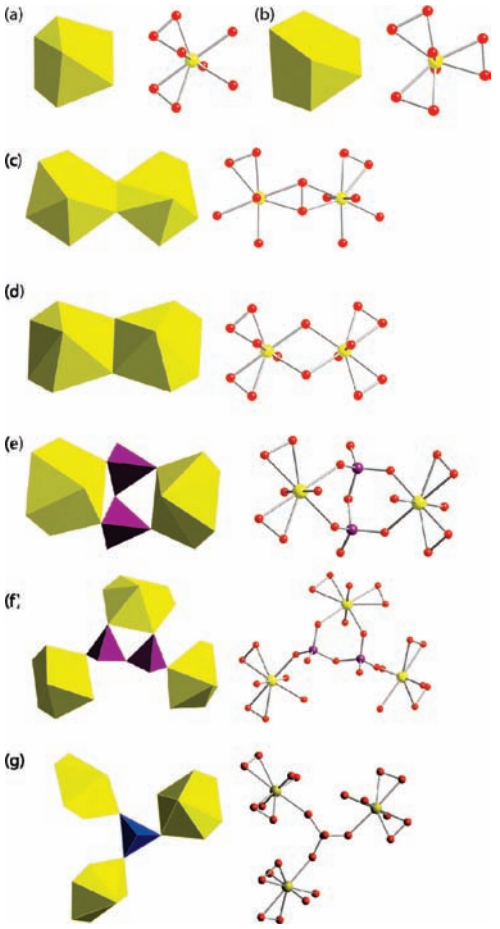

Figure 1. Coordination environments of uranyl ions in the five cage clusters examined here. Uranyl polyhedra and U atoms are shown in yellow, phosphate tetrahedra and P atoms are in blue, and O atoms are shown as red balls.

The cage clusters reported here present several local environments about uranyl ions. These are summarized in Figure 1. All of the U^{6+} is present in all of the clusters as linear (or nearly so) $(UO_2)^{2+}$ uranyl ions. These are further coordinated to create uranyl hexagonal bipyramids with the apexes defined by the O atoms of the uranyl ions. In all cases, uranyl ion U^{6+}—O bond lengths are ~1.8 Å, and peroxide O—O bond lengths are ~1.45—1.5 Å. In some of these hexagonal bipyramids, hereafter designated diperoxide hexagonal bipyramids, two of the equatorial edges of the bipyramid correspond to bidentate peroxide groups (Figure 1a). In other cases, the uranyl hexagonal bipyramids have three equatorial edges defined by peroxide and are hereafter designated triperoxide hexagonal bipyramids (Figure 1b). The bridges between uranyl ions where bipyramids share an edge are either peroxide groups or two hydroxyl groups (Figures 1c,d). In three of the clusters, pyrophosphate groups bridge between uranyl ions. The uranyl ion may be coordinated by a pyrophosphate group, such that two adjacent equatorial vertices of the hexagonal bipyramid correspond to O atoms of a pyrophosphate group, with one of the O atoms being from each of the two phosphate tetrahedra (Figure 1e). In other cases, a

dx.doi.org/10.1021/ic200065y |*Inorg. Chem.* 2011, 50, 5509–5516

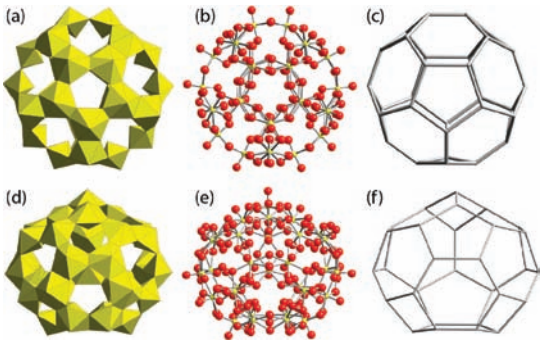

Figure 2. Polyhedral (a,d), ball-and-stick (b,e), and graphical representations (c,f) of cluster U_{30a}. Uranyl polyhedra and U atoms are shown in yellow, and O atoms are colored red. Each vertex in the graphical representation corresponds to a U atom, and lines designate shared edges between polyhedra about the corresponding U atoms.

uranyl ion is linked to a single phosphate tetrahedron by sharing an equatorial vertex. This tetrahedron may be isolated or part of a pyrophosphate group (Figure 1f,g).

Cluster U_{30a} contains 30 uranyl diperoxide hexagonal bipyramids and is distinct from the U_{30} cluster that we reported earlier (Figure 2a−f). Each of the bipyramids contains two hydroxyl groups that define an equatorial edge. Bipyramids share edges that are defined by peroxide groups and also by two hydroxyl groups, and each bipyramid shares edges with three other bipyramids. The result is a cluster with composition $[(UO_2)_{30}(O_2)_{30}(OH)_{30}]^{30-}$. The dimensions of the cage cluster, which is a flattened sphere, are 22.2 by 18.3 Å, measured from the outer edges of bounding O atoms.

Cluster U_{30a} has ideal symmetry C_{5v} and is the first cage cluster built from uranyl bipyramids that has a 5-fold rotational axis. Graphical representations of the topology are provided in Figure 2c,f. Vertices in the graph correspond to U atoms, and lines represent edges that are shared between uranyl hexagonal bipyramids. The graph, with 30 vertices, contains five squares, two pentagons, and 10 hexagons. The cluster contains five Ba cations and two Rb cations, inside the squares and pentagons of the topology, respectively. The remaining charge of the cluster, −18, is balanced by Li cations and partially occupied Rb cations outside the clusters.

The $U_{30}Py_6$ cluster contains 18 uranyl triperoxide hexagonal bipyramids, 12 uranyl diperoxide hexagonal bipyramids, and six pyrophosphate groups. In the cases where a uranyl ion is coordinated by two bidentate peroxide groups, an additional equatorial edge corresponds to two O atoms of a given pyrophosphate group, with the linkage illustrated in Figures 1e and 3a,c. The cluster has composition $[(UO_2)_{30}(O_2)_{39}(P_2O_7)_6]^{42-}$ with disordered charge balancing K^+ atoms located both inside and outside the cluster. The infrared spectrum indicates that tartaric acid contained in the synthesis was not incorporated in the crystals. The cluster has dimensions 23.0 by 19.5 Å, as measured from the outer edges of bounding O atoms. The inclusion of six pyrophosphate groups noticeably increased the size of the cluster, relative to U_{30a}. The inclusion of pyrophosphate also increases the charge of the cage cluster significantly (from −30 to −42) and presents a means to tune the cluster radius/charge ratio.

Graphical representations of cluster $U_{30}Py_6$ are given in Figure 3b,d. Each vertex of the graph represents a U atom.

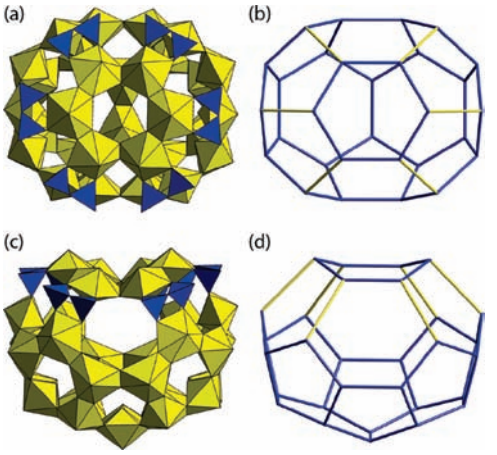

Figure 3. Polyhedral (a,c) and graphical representations (b,c) of cluster $U_{30}Py_6$. Uranyl and phosphate polyhedra are shown in yellow and blue, respectively. Each vertex in the graphical representation corresponds to a U atom, blue lines designate shared edges between polyhedra about the corresponding U atoms, and yellow lines indicate bridges through pyrophosphate tetrahedra.

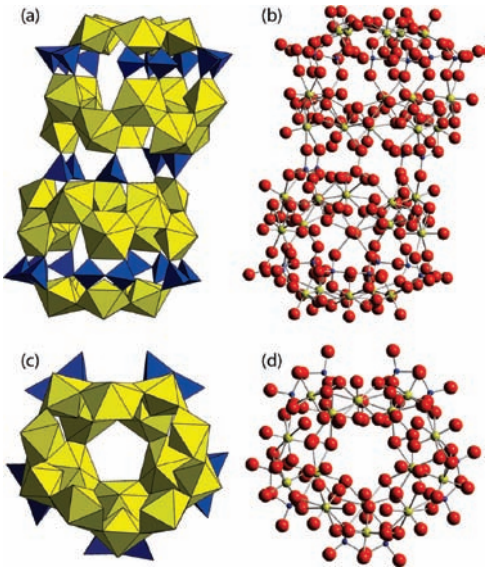

Figure 4. Polyhedral (a,c) and ball-and-stick representations (b,d) of cluster $U_{30}Py_{12}P_1$. Uranyl and phosphate polyhedra are shown in yellow and blue, respectively. O, U, and P atoms are colored red, yellow, and blue, respectively.

Where uranyl polyhedra share an equatorial edge, the linkage is indicated by a blue connector between the vertices that correspond to these uranyl ions. Six pyrophosphate groups bridge between uranyl polyhedra in the cluster. In the graphical representations, this is shown as a yellow line drawn between the two vertices that correspond to the U atoms. Note that pyrophosphate groups do not have corresponding vertices in the graph. The graphical representations reveal that the cluster topology consists of 12 pentagons and five hexagons. It is a fullerene topology, as are several other cage clusters built from uranyl polyhedra and pyrophosphate groups.

Polyhedral representations of cluster $U_{30}Py_{12}P_1$, which exhibits several novel features, are shown in Figure 4. All of the

dx.doi.org/10.1021/ic200065y |*Inorg. Chem.* 2011, 50, 5509–5516

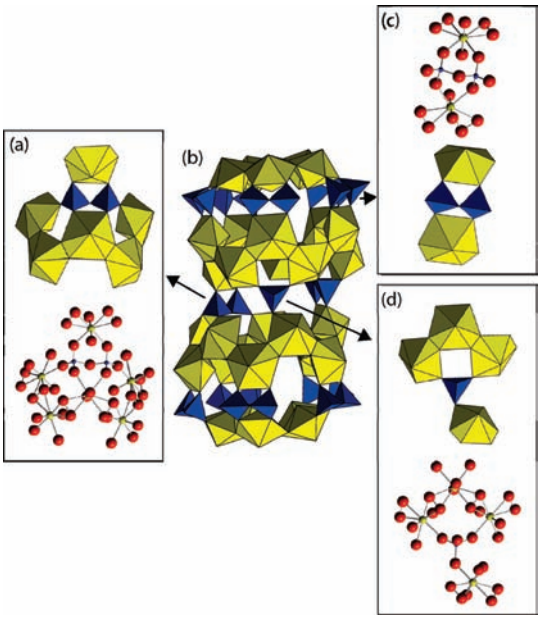

Figure 5. Polyhedral and ball-and-stick representations of cluster $U_{30}Py_{12}P_1$. Legend as in Figure 4.

uranyl hexagonal bipyramids contain two peroxide groups located along equatorial edges. The other two equatorial ligands correspond to O atoms of pyrophosphate groups or O atoms of phosphate tetrahedra or are H_2O groups.

The linkages about the phosphate and pyrophosphate groups in $U_{30}Py_{12}P_1$ are extraordinary. Ten of the pyrophosphate groups share four of their O atoms with two different uranyl hexagonal bipyramids, such that an equatorial edge of each bipyramid is defined by two of these O atoms (Figure 5c). This particular linkage between uranyl bipyramids and pyrophosphate groups has been reported earlier in eight different clusters.[20] There are two additional pyrophosphate groups in $U_{30}Py_{12}P_1$ that present novel connectivities (Figure 5a). These are located toward the center of the cluster, and each shares all six of its nonbridging O atoms with four different uranyl bipyramids. Cluster $U_{30}Py_{12}P_1$ is also the first we have created that contains an isolated phosphate tetrahedron, and in the cluster, this shares three of its O atoms with three different uranyl bipyramids (Figure 5d).

Each of the uranyl hexagonal bipyramids in $U_{30}Py_{12}P_1$ shares all of its edges that are defined by peroxide groups with other uranyl bipyramids. The cluster is elongated, with each end truncated by a five-membered ring of edge-sharing bipyramids. Two distinct lobes are evident in the cluster, and each contains a 10-membered ring of edge-sharing uranyl bipyramids. These 10-membered rings are linked to the five-membered rings that truncate the cluster on either end through bridging pyrophosphate units.

The two lobes of cluster $U_{30}Py_{12}P_1$ are identical but are twisted relative to each other. They are connected through two pyrophosphate groups and a single phosphate tetrahedron. One of these pyrophosphate groups shares four O atoms with three adjacent uranyl bipyramids in one lobe and two O atoms with a single uranyl bipyramid in the other lobe. The other pyrophosphate group has the same connectivity except in a reverse direction. The single phosphate tetrahedron bridges between uranyl bipyramids in one lobe by sharing one O atom with each and is linked to one bipyramid of the other lobe through a single

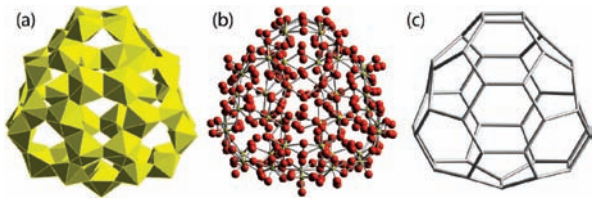

Figure 6. Polyhedral (a), ball-and-stick (b), and graphical representations (c) of cluster U_{42}. Legend as in Figure 2.

O atom. Note that four of the bipyramids, two from either lobe, contain a H_2O at an equatorial vertex that is not shared with another bipyramid, phosphate, or pyrophosphate group. This is the first cage cluster built from uranyl bipyramids that we have found with nonbridging equatorial vertices in any bipyramids, although we earlier reported two crown-shaped clusters and one bowl-shaped cluster built from uranyl hexagonal bipyramids that have several nonbridging equatorial O atoms.[24]

The complex cluster $U_{30}Py_{12}P_1$ has the composition $[(UO_2)_{30}(O_2)_{30}(P_2O_7)_{12}(PO_4)(H_2O)_5]^{51-}$, and the charge of the cluster is presumably balanced by K^+ and Li^+ cations located both inside and outside the cluster. 2,3-Dihydroxybutanedioic acid cations present in the synthesis were probably not incorporated in the crystals, as they are not apparent in the infrared spectra. The cluster dimensions are 28.8 by 18.7 Å, as measured from the outer edges of bounding O atoms.

Considering bridges between uranyl polyhedra through phosphate tetrahedra to be equivalent to shared edges between the bipyramids, cluster $U_{30}Py_{12}P_1$ contains 12 topological pentagons and six hexagons. It is therefore a fullerene topology, although it is not the same isomer as $U_{30}Py_6$.

The U_{42} cluster is built from 42 uranyl diperoxide hexagonal bipyramids, each of which contain two OH groups that define an equatorial edge (Figure 6). This is the first cluster we have found that contains 42 uranyl polyhedra, although it is built from the same type of uranyl hexagonal bipyramids as several other cage clusters we have reported. There are 21 crystallographically unique uranyl ions within the cluster. The cluster composition is $[(UO_2)_{42}(O_2)_{42}(OH)_{42}]^{42-}$. There are K^+ cations located below each five-member ring of bipyramids in the cluster, and an ordered Li^+ cation is located below the center of each four-member ring of bipyramids. Disordered Li^+ cations outside the cluster balance the remaining −31 charge of the cluster. U_{42} is somewhat flattened with maximum and minimum dimensions of 25.0 and 23.0 Å, as measured from the outer edges of bounding O atoms.

The graphical representation of cluster U_{42}, defined as for U_{30} above, is shown in Figure 6c. The topology contains three squares, six pentagons, and 14 hexagons. It has ideal symmetry D_{3h}.

The $U_{42}Py_3$ cluster, which is closely related topologically to U_{42}, contains 42 uranyl hexagonal bipyramids and three pyrophosphate groups (Figure 7b,d). Thirty-six of the bipyramids contain two peroxide groups arranged along equatorial edges, with a third edge of each defined by two OH groups. The remaining six uranyl hexagonal bipyramids each contain two peroxide groups along equatorial edges, as well as two O atoms of pyrophosphate groups that define another equatorial edge.

Note that the topology of $U_{42}Py_3$ is identical to that of U_{42} (Figure 7) and that $U_{42}Py_3$ is a derivative of U_{42} achieved by replacing three of the shared equatorial edges of uranyl

dx.doi.org/10.1021/ic200065y |*Inorg. Chem.* 2011, 50, 5509–5516

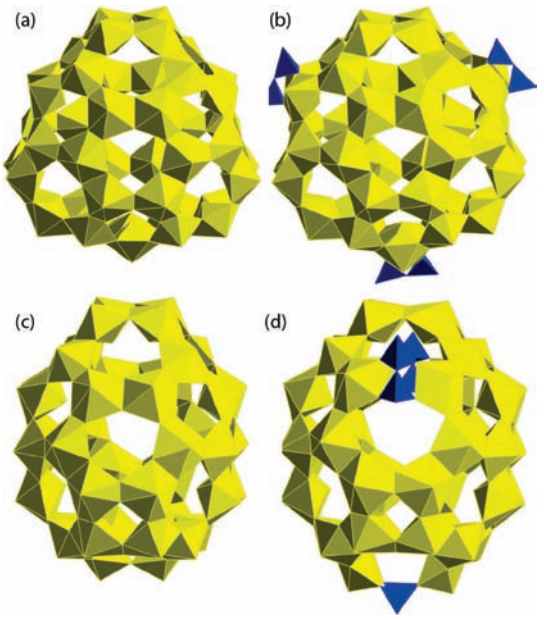

Figure 7. Polyhedral representations of clusters U_{42} (a,c) and $U_{42}P_3$ (b,d). Legend as in Figure 3.

bipyramids that correspond to two OH groups by three pyrophosphate groups. The composition of $U_{42}Py_3$ is $[(UO_2)_{42}(O_2)_{42}(OH)_{36}(P_2O_7)_3]^{48-}$, with K^+ cations located below the centers of five- and six-membered rings of bipyramids. The net charge of −36 is balanced by disordered Li^+ cations located between the clusters in the crystal. Oxalic acid was included in the synthesis, but the infrared spectrum indicates it was not incorporated into the crystal.

Topological Isomers. There are 227 graphs containing 30 three-connected vertices that have at least one square and any number of pentagons and hexagons. These are assigned numerical designations by the CaGe program. Cluster U_{30}, which we previously reported,[19] adopts graph 44. Cluster U_{30a} of the current study adopts number 88.

Including those of the current study, we have reported 11 cage clusters built from uranyl polyhedra that contain topological squares. Topological squares are never adjacent to topological pentagons or squares in these clusters. In other words, all four edges of topological squares in cage clusters of uranyl polyhedra are most often shared with adjacent hexagons and, in one case, with a topological octagon. This observation will be discussed further below but, for the moment, can be used to place restrictions on the subset of the 227 graphs that warrant further consideration. Of the 227 graphs, only numbers 44, 61, 69, 88, and 130 have no square−square or square−pentagon adjacencies. These are shown in Figure 8. Graphs 44, 61, 69, 88, and 130 contain from one to six squares (1, 2, 3, 5, or 6). In general, they have higher symmetry arrangements than the other graphs with 30 vertices.

The graphical representations of the topologies of clusters $U_{30}Py_6$ and $U_{30}Py_{12}P_1$ contain only pentagons and hexagons and are fullerene topologies. There are only three possible fullerene topologies that contain 30 vertices.[28] With reference to the order of these graphs in Figure 8, cluster $U_{30}Py_6$ adopts the first and $U_{30}Py_{12}P_1$, the third.

There are 2373 graphs with 42 three-connected vertices that contain at least one square and any number of pentagons and hexagons in their topologies. There are 39 that contain exactly three topological squares and that have no square−square or square−pentagon adjacencies. The graph adopted by U_{42} and $U_{42}Py_3$ (number 177), with point group symmetry D_{3h} has the highest symmetry of the 39 graphs. Two of these graphs have C_{2v} symmetry, and the remainder contain fewer symmetry operators (Figure 9).

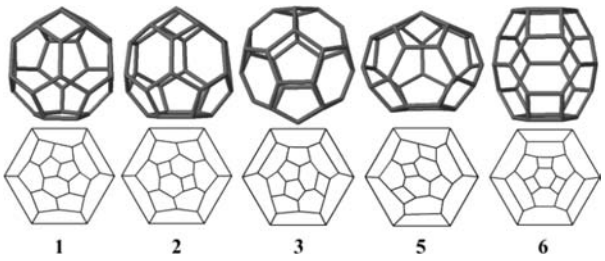

Figure 8. Three-connected graphs containing 30 vertices, at least one square, and no square−square or square−pentagonal adjacencies. The corresponding Schlegel diagrams are given underneath the three-dimensional representations of each graph. The number beneath the Schlegel graph indicates the number of squares present in the topology.

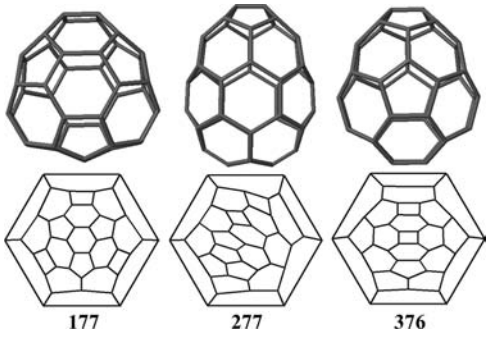

Figure 9. Graphical representations of a selection of graphs that contain 42 vertices, at least one topological square, and no square−square or square−pentagonal adjacencies. The top portion contains representations of the graphs in three dimensions, and the bottom corresponds to Schlegel representations of the graph. Graph 177 is the topology adopted by U_{42}, whereas 277 and 376 represent the two graphs with the next highest symmetry, C_{2v}.

Infrared Spectroscopy. The infrared spectra obtained using an ATR objective for a crushed crystal corresponding to each cluster are collected in Figure 10. Modes in the range of 800−900 cm^{-1} arise from the uranyl ions. Four modes in the range of 980−1150 cm^{-1} are attributed to the pyrophosphate groups. Water bending modes are present at about 1630 cm^{-1}, and H bonds are indicated by the broad envelope extending from about 2900 to 3650 cm^{-1} in each spectrum.

DISCUSSION

The current study further expands the suite of cage clusters that we have created using uranyl polyhedra and demonstrates that properties such as cluster radius and charge ratios can be selected. Likewise, pore spaces in the walls of the clusters can be tuned to different sizes by using various linkers, including pyrophosphate and oxalate. The five clusters reported herein demonstrate again that uranyl pyrophosphate cage clusters can be topological derivatives of clusters that contain only uranyl polyhedra, or they can adopt novel topologies.

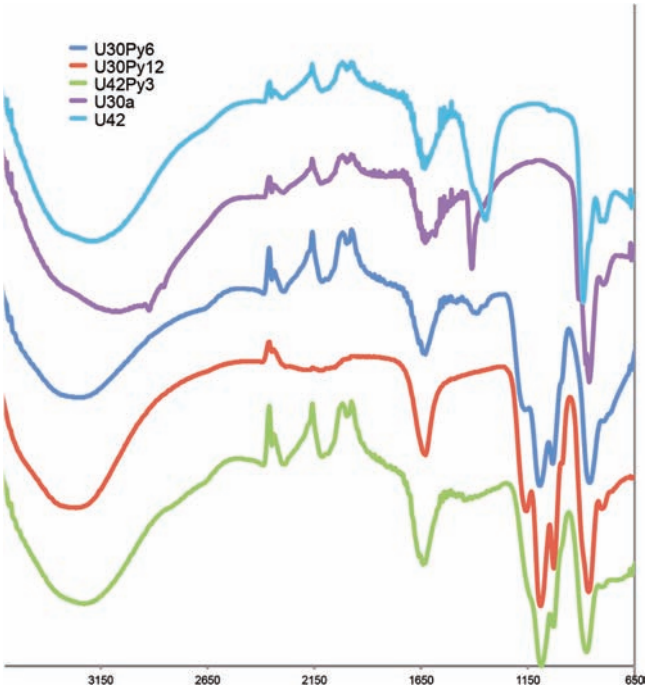

Figure 10. Infrared spectra for crystals containing each cluster. X-axis: cm^{-1}; Y-axis: Arbitrary intensity.

Having accumulated 11 cage clusters built from uranyl polyhedra that contain topological squares, it is apparent that the topologies adopted by these clusters do not contain square−square or square−pentagon adjacencies, whereas square−hexagon adjacencies are indispensible.

Where topological squares occur in cage clusters built from uranyl bipyramids, they are built from four diperoxide polyhedra. The edges of the square correspond to four peroxide bridges. There are four edges that are each defined by two OH groups that are not shared within the square. These OH−OH edges are shared with adjacent polyhedra within the cage cluster and thus correspond to edges of other polygons that are adjacent to squares in the corresponding graphs.

In the case of a topological square, geometric constraints require that the shared edges be peroxide. The O−O separation of an OH−OH edge is ∼2.8 Å, and bridging uranyl ions through an OH−OH edge within the topological square would result in O−O separations across the ring of less than 2.5 Å, which is prohibitively short. If uranyl diperoxide polyhedra are connected into cage clusters, there will be no adjacent squares in the topology. If the cluster is built from uranyl triperoxide polyhedra, topological squares would not be prohibited, but the clusters we have created to date that are built from exclusively triperoxide polyhedra contain no topological squares.

The edges of topological pentagons within the known cage clusters built from uranyl polyhedra correspond to either five peroxide bridges or four peroxide bridges and one OH−OH bridge. Topological hexagons have been observed in which six, four, or three edges correspond to peroxide bridges, with the others being OH−OH bridges.

It is currently unclear as to why square−pentagon adjacencies are absent in the topologies of cage clusters built from uranyl polyhedra. It is geometrically possible to place as many as four pentagons at the edges of a square such that adjacent pentagons share an edge, although more curvature is needed than if the square is surrounded by hexagons. The arrangement of four hexagons around a square permits 4-fold symmetry in four of the clusters we have created, and in general locating hexagons adjacent to squares produces more symmetric topologies than if one or more of the hexagons is replaced by a pentagon. However, the relative stabilities of different topological arrangements of uranyl polyhedra in cage clusters awaits computational studies.

■ ASSOCIATED CONTENT

Supporting Information. Tables of crystal data, atomic coordinates and isotropic displacement parameters, bond lengths, and anisotropic displacement parameters. This material is available free of charge via the Internet at http://pubs.acs.org.

■ AUTHOR INFORMATION

Corresponding Author
*E-mail: pburns@nd.edu.

■ ACKNOWLEDGMENT

This material is based upon work supported as part of the Materials Science of Actinides Center, an Energy Frontier Research Center funded by the U.S. Department of Energy, Office of Science, Office of Basic Energy Sciences under Award Number DE-SC0001089.

■ REFERENCES

(1) Long, D. L.; Burkholder, E.; Cronin, L. *Chem. Soc. Rev.* **2007**, *36*, 105–121.
(2) Long, D. L.; Tsunashima, R.; Cronin, L. *Angew. Chem., Int. Ed.* **2010**, *49*, 1736–1758.
(3) Mitchell, S. G.; Streb, C.; Miras, H. N.; Boyd, T.; Long, D. L.; Cronin, L. *Nature Chem.* **2010**, *2*, 308–312.
(4) Yan, J.; Long, D. L.; Cronin, L. *Angew. Chem., Int. Ed.* **2010**, *49*, 4117–4120.
(5) Kroto, H. W.; Heath, J. R.; Obrien, S. C.; Curl, R. F.; Smalley, R. E. *Nature* **1985**, *318*, 162–163.
(6) Xie, S. Y.; Gao, F.; Lu, X.; Huang, R. B.; Wang, C. R.; Zhang, X.; Liu, M. L.; Deng, S. L.; Zheng, L. S. *Science* **2004**, *304*, 699–699.
(7) Burns, P. C.; Ikeda, Y.; Czerwinski, K. *MRS Bull.* **2010**, *35*, 868–876.
(8) Antonio, M. R.; Chiang, M. H. *Inorg. Chem.* **2008**, *47*, 8278–8285.
(9) Berthet, J. C.; Thuery, P.; Ephritikhine, M. *Angew. Chem., Int. Ed.* **2008**, *47*, 5586–5589.
(10) Choppin, G. R.; Wall, D. E. *J. Radioanal. Nuclear Chem.* **2003**, *255*, 47–52.
(11) Craciun, C.; Rusu, D.; Pop-Fanea, L.; Hossu, M.; Rusu, M.; David, L. *J. Radioanal. Nuclear Chem.* **2005**, *264*, 589–594.
(12) Gaunt, A. J.; May, I.; Collison, D.; Holman, K. T.; Pope, M. T. *J. Mol. Struct.* **2003**, *656*, 101–106.
(13) Gaunt, A. J.; May, I.; Copping, R.; Bhatt, A. I.; Collison, D.; Fox, O. D.; Holman, K. T.; Pope, M. T. *Dalton Trans.* **2003**, 3009–3014.
(14) Gaunt, A. J.; May, I.; Helliwell, M.; Richardson, S. *J. Am. Chem. Soc.* **2002**, *124*, 13350–13351.
(15) Khoshnavazi, R.; Eshtiagh-Hossieni, H.; Alizadeh, M. H.; Pope, M. T. *Polyhedron* **2006**, *25*, 1921–1926.
(16) Burns, P. C.; Kubatko, K. A.; Sigmon, G.; Fryer, B. J.; Gagnon, J. E.; Antonio, M. R.; Soderholm, L. *Angew. Chem., Int. Ed.* **2005**, *44*, 2135–2139.
(17) Forbes, T. Z.; McAlpin, J. G.; Murphy, R.; Burns, P. C. *Angew. Chem., Int. Ed.* **2008**, *47*, 2824–2827.

(18) Sigmon, G.; Ling, J.; Unruh, D. K.; Moore-Shay, L.; Ward, M.; Weaver, B.; Burns, P. C. *J. Am. Chem. Soc.* **2009**, *131*, 16648–16649.
(19) Unruh, D. K.; Burtner, A.; Pressprich, L.; Sigmon, G.; Burns, P. C. *Dalton Trans.* **2010**, *39*, 5807–5813.
(20) Ling, J.; Qiu, J.; Sigmon, G. E.; Ward, M.; Szymanowski, J. E. S.; Burns, P. C. *J. Am. Chem. Soc.* **2010**, *132*, 13395–13402.
(21) Ling, J.; Wallace, C. M.; Szymanowski, J. E. S.; Burns, P. C. *Angew. Chem., Int. Ed.* **2010**, *49*, 7271–7273.
(22) Vlaisavljevich, B.; Gagliardi, L.; Burns, P. C. *J. Am. Chem. Soc.* **2010**, *132*, 14503–14508.
(23) Sigmon, G. E.; Unruh, D. K.; Ling, J.; Weaver, B.; Ward, M.; Pressprich, L.; Simonetti, A.; Burns, P. C. *Angew. Chem., Int. Ed.* **2009**, *48*, 2737–2740.
(24) Sigmon, G. E.; Weaver, B.; Kubatko, K. A.; Burns, P. C. *Inorg. Chem.* **2009**, *48*, 10907–10909.
(25) Sheldrick, G. M. *SHELXTL*, version 6.12; Bruker AXS, Inc.: Madison, WI, 1996.
(26) Burns, P. C.; Ewing, R. C.; Hawthorne, F. C. *Can. Mineral* **1997**, *35*, 1551–1570.
(27) Brinkman, G.; Delado, O.; Friedrichs, S.; Lisken, S.; Peeters, A.; Van Cleemput, N. *MATCH Commun. Math. Comput. Chem.* **2010**, *63*, 533–552.
(28) Fowler, P.; Manolopoulos, D. *An Atlas of Fullerenes*, 2nd ed.; Dover Publications, Inc.: Mineola, NY, 2006; p 392.